

## High Energy, High Resolution, X-ray Studies of the Structure of Complex Materials

Simon J. L. Billinge<sup>1</sup>, Valeri Petkov<sup>1</sup>, and Stefan Kycia<sup>2</sup>

<sup>1</sup>Department of Physics and Astronomy, Michigan State University, East Lansing, MI 48823

<sup>2</sup>Laboratorio Nacional de Luz Sincrotron, Campinas, Brazil

Real crystals are not perfect, defect-free, long-range ordered arrays of atoms, but contain imperfections. The crystal properties are strongly affected (and to some extent determined) by the defects. For example, semiconductors become metallic when doped with non-isovalent impurities and it is the presence of defects (dislocations) that make metals malleable. A quote attributed to F. C. Franck says “crystals are like people, it is their defects that make them interesting” and this is an idea that is made use of by materials physicists and chemists. Modern functional materials increasingly take advantage of low dimensionality, confined geometries, and disorder to yield useful properties.

Defects in crystals give rise to diffuse scattering that is difficult to measure and analyze quantitatively. We have developed quantitative methods for analyzing highly defective crystals using real-space methods [1-11]. The approach is old and was used as early as the 1930's by B.E. Warren [12] to study carbon blacks. With the advent of large fluxes of high-energy x-rays at synchrotrons such as CHESS, APS, and ESRF, coupled with advances in computing, these experiments are yielding unprecedented detail and quantitative information about defects in crystalline materials. A real-space resolution that is sub-atomic ( $\Delta r \sim 0.12 \text{ \AA}$ ) and sample-limited has now been achieved from x-ray measurements. This was not thought possible because of the x-ray atomic scattering factor that kills scattering intensity at high momentum transfers. The very high flux of high energy photons at the A2 wiggler line at CHESS allowed these problems to be overcome. The flexibility of the CHESS beamlines and help and responsiveness of the staff were also critical factors in the development of these novel experiments, which are now carried out at other facilities as well as CHESS.

We present examples below. A promising new frontier is now developing from this work that we term

“nanocrystallography”: the determination of the structure of materials where the structural coherence is limited to the 1-10 nm length-scale. A growing number of materials fit into this category. Their structure, a prerequisite for understanding their properties in detail, cannot be solved using conventional methods because of the absence of Bragg peaks due to the limited structural coherence. Using the methods we describe here, this problem is being overcome.

The first experiments where the very high real-space resolution was demonstrated were carried out on semiconductor alloys. These are technologically important materials valued for their wide applications in optoelectronic devices such as lasers and detectors [13]. By varying composition the band-gap and lattice can be independently and continuously varied. The alloying introduces substantial structural disorder that, despite its importance, has not been properly characterized. Employing high energy powder diffraction and the atomic pair distribution function (PDF) technique at CHESS for the first time we resolved bond-lengths of In-As and Ga-As in  $\text{In}_{1-x}\text{Ga}_x\text{As}$  differing by  $\Delta r = 0.14 \text{ \AA}$  [10]. Both the local and intermediate range structures were successfully determined using a supercell model based on the Kirkwood potential. Details can be found in [2,3,8,10]. Data were collected at beamline A2 at CHESS at 60keV energy ( $\lambda = 0.206 \text{ \AA}$ ) over a wide angular range from uniform powders. The data are corrected for experimental effects and put on an absolute scale before Fourier transforming to real-space to recover the PDF,

$$\Delta(r) = \frac{2}{\pi} \int_0^\infty Q[S(Q) - 1] \sin(Qr) dQ.$$

PDFs from the alloy series are shown in Fig. 1. The doublet at  $r \sim 2.5 \text{ \AA}$  in the alloys shows the resolved short Ga-As and long In-As bonds (peaks in the PDF appear at distances corresponding to atom separations in the solid). These peak positions do not correspond to the

average bond length determined crystallographically. Rather, it appears that locally the bonds are either short Ga-As bonds or long In-As bonds depending on which ion resides on a particular lattice site. This clearly demonstrates that the PDF is sensitive to the real local bonding.

The intermediate range structure (4 – 15 Å), on the other hand is highly strained and behaves much more like the average structure. For example, the doublet at 12 Å in Fig. 1 does not become a quadruplet in the alloys but stays a broadened doublet that smoothly interpolates between the respective positions in the end-members, behavior distinct from that of the nearest neighbor peak. We found that most of the strain relaxation occurs on the As sublattice. Modeling these data using a Kirkwood model allowed us to extract the average atomic probability-distribution-function (this is the static equivalent of the thermal ellipsoid used in crystallography) on the As site. This is highly directional and non Gaussian, as shown in Fig. 2. The directionality is straightforwardly understood from the underlying geometry [3].

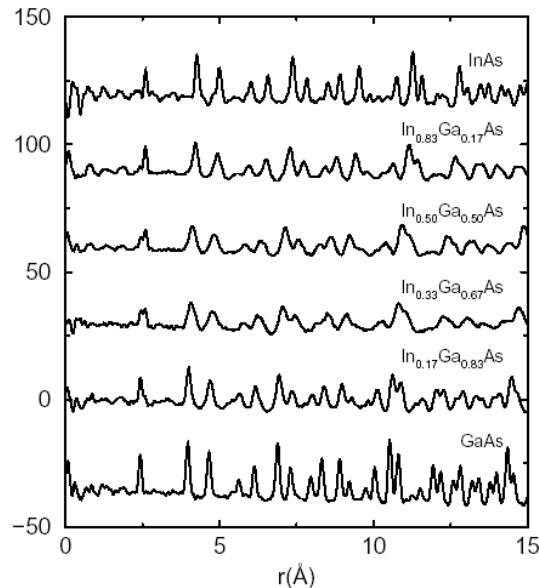


**Fig. 1** The reduced PDF,  $G(r)$  for  $\text{In}_{1-x}\text{Ga}_x\text{As}$  measured at 10 K. The data-sets are offset for clarity. In the alloy PDFs the first-neighbor peak is seen to be split into a doublet coming from the local In-As and Ga-As bonds, respectively, that are present in the alloy.

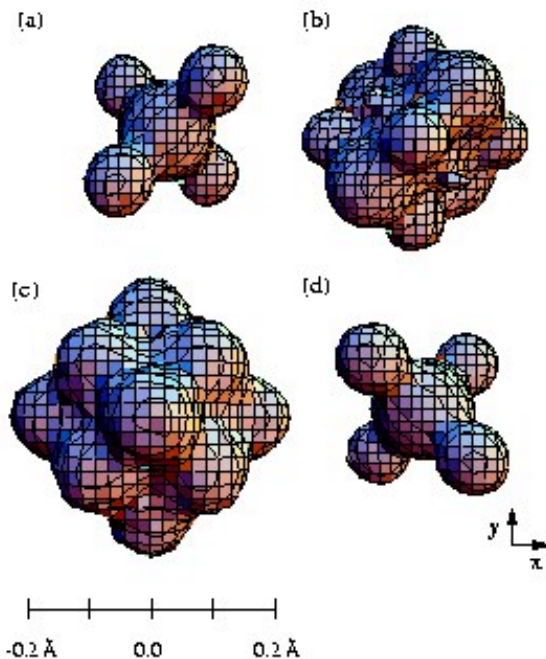


**Fig. 2** Iso-probability surface for the ensemble averaged As atom distribution. The surfaces plotted all enclose the volume where As atoms will be found with 68 % probability. (a)  $\text{In}_{0.17}\text{Ga}_{0.83}\text{As}$  (b)  $\text{In}_{0.33}\text{Ga}_{0.67}\text{As}$  (c)  $\text{In}_{0.50}\text{Ga}_{0.50}\text{As}$  (d)  $\text{In}_{0.83}\text{Ga}_{0.17}\text{As}$ . In each case, the probability distribution is viewed down the [001] axis

High real-space resolution x-ray PDFs have now been applied in a number of different studies, for example, polaron formation in colossal magnetoresistant manganites [4,9], nanocrystalline [5] and conducting polymers [11] and imperfectly crystallized small organic molecules [14]. Each of these studies were carried out at CHESS. Technical developments continue at CHESS with the prototyping of a custom designed, energy resolving, multi-element linear array detector that was used in the last study on molecular systems. These are particularly challenging because of the low-Z nature of the constituents that results in relatively weak elastic scattering on a relatively strong incoherent (Compton) scattering background. This is not so acute for Bragg-scattering but presents a technical challenge in the case of diffuse scattering measurements. The problems are surmountable as demonstrated by a PDF study of silica glasses [15] and the data from the organics [14].

Having developed the experimental techniques at CHESS we have carried out experiments at other facilities and a beamline optimized for high energy, wide angle, powder diffraction is being built at APS sector 6. The approaches outlined here lend themselves to materials with limited structural coherence, or constrained in confined geometries, loosely described

## Research Highlight

as “nanocrystallography”. More recent representative examples are shown in Figures 3 and 4. The case of  $\text{LiMoS}_2$  is shown in Fig. 3 [16]. The intercalated  $\text{Li}^+$  ions reduce the Mo allowing 3-fold metal-metal bonding. The  $\text{MoS}_2$  layer rearranges from regular hexagons of Mo to chains of metal-metal bonded, triply coordinated,  $\text{Mo}_3$  motifs that propagate through the structure. The structure was solved for the first time from the PDFs shown in Figure 3. The insets show that, while pristine  $\text{MoS}_2$  is a well-ordered crystal (peaks in the PDF extend indefinitely), the structural coherence of  $\text{LiMoS}_2$  is limited to  $\sim 50\text{\AA}$ . In the other example (Fig. 4) the structure of Cs intercalated in the pores of the zeolite ITQ-4 was determined [17]. A differential technique was used where the scattering from the host matrix was subtracted. The PDFs shown are the differential PDFs of just the Cs ions. By modeling this it was shown that Cs forms broken zig-zag chains of  $\text{Cs}^+$  ions. Charge balance is provided by an electron gas that resides in the cavities, and this is an example of an inorganic “electride” [17]. The electron gas is low dimensional and highly correlated, behaving like a Mott insulator [16].

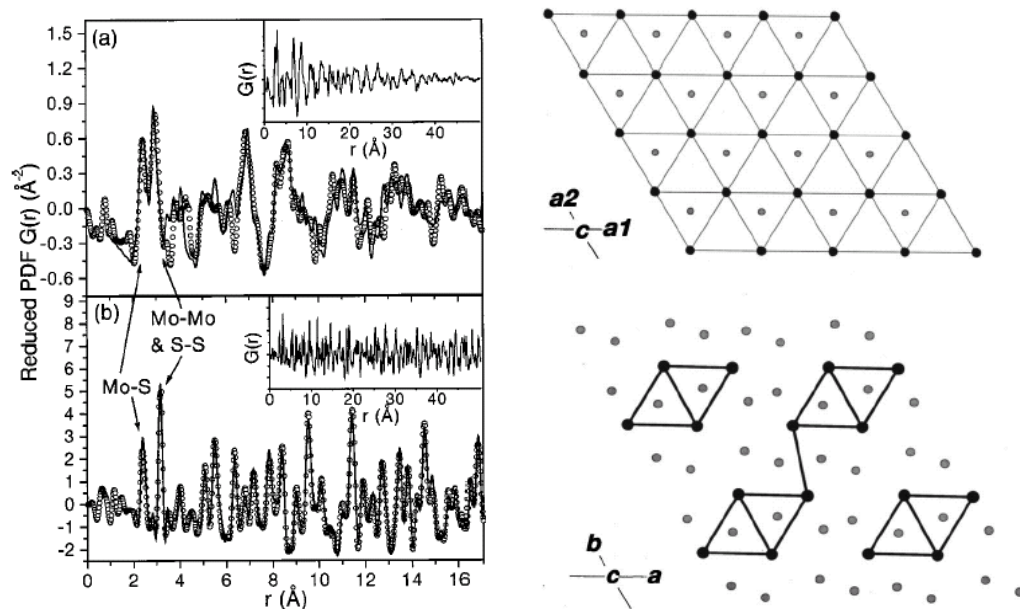


**Fig. 3** Comparison between the experimental PDF for  $\text{LiMoS}_2$  (circles) and model PDF's (line) for  $\text{LiMoS}_2$  (top panel) and  $\text{MoS}_2$  (bottom panel). Projections down the  $c$ -axis of the resulting models are also shown. The regular hexagonal array of Mo ions in  $\text{MoS}_2$  (above) are displaced and rearranged in  $\text{LiMoS}_2$  (bottom) [16].

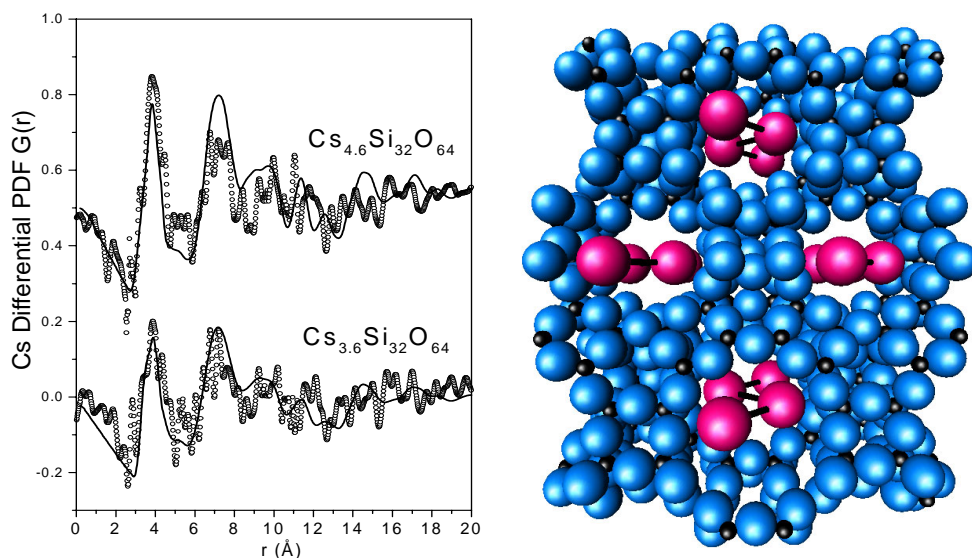
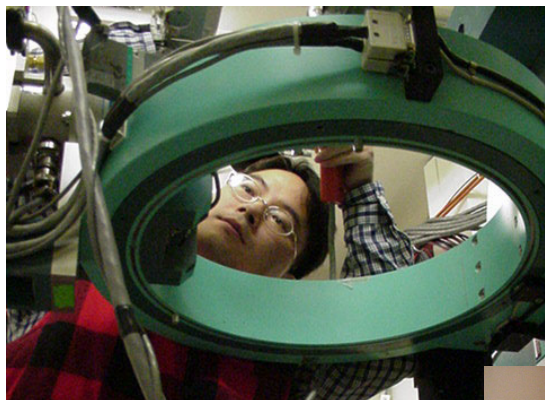


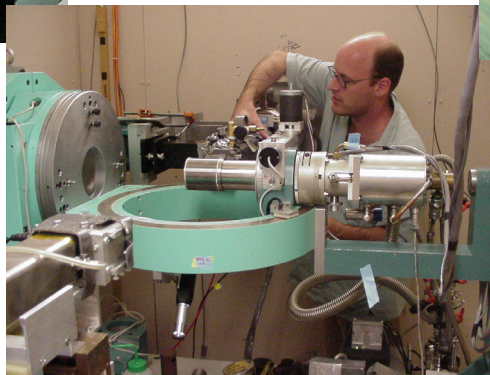
**Fig. 4** Differential PDFs (with the host scattering subtracted) showing the structure of Cs intercalated in ITQ-4. Modeling the total and differential PDFs indicates that the intercalated Cs is in the form of  $\text{Cs}^+$  ions arranged in broken zig-zag chains as shown on the right [17].



Il-Young Jeong (grad student) at A2



Simon Billinge in his lab at MSU



Stefan Kycia at A2

Finally, we would like to thank funding agencies for their support: DOE through DE-FG02-97ER45651 and NSF through DMR-0075149 and CHE-9903706, as well as the warm hospitality and help of the CHESS staff, not least Stefan Kycia and Randy Headrick.

#### References

- [1] V. Petkov and S. J. L. Billinge, From crystals to nanocrystals: semiconductors and beyond, In *From semiconductors to proteins: beyond the average structure*, (Kluwer/Plenum, New York, 2001), M. F. Thorpe and S. J. L. Billinge, Eds.
- [2] V. Petkov and S. J. L. Billinge, Local structure of random  $\text{In}_x\text{Ga}_{1-x}\text{As}$  alloys by full-profile fitting of atomic pair distribution functions, *Physica B*, **305**, 83 (2001).
- [3] I.-K. Jeong, F. Mohiuddin-Jacobs, V. Petkov, S. J. L. Billinge and S. Kycia, Local structure study of  $\text{In}_x\text{Ga}_{1-x}\text{As}$  semiconductor alloys using high energy synchrotron x-ray diffraction, *Phys. Rev. B* **63**, 205202 (2001).
- [4] S. J. L. Billinge, V. Petkov, Th. Proffen, G. H. Kwei, J. L. Sarrao, S. D. Shastri and S. Kycia, Charge inhomogeneities in the colossal magnetoresistant manganites from the local atomic structure, *Mater. Res. Soc. Symp. Proc.* **602**, 177 (2001).
- [5] V. Petkov, S. J. L. Billinge, J. Heising and M. G. Kanatzidis, Application of atomic pair distribution function analysis to materials with intrinsic disorder. Three-dimensional structure of exfoliated-restacked  $\text{WS}_2$ : Not just a random turbostratic assembly of layers, *J. Am. Chem. Soc.* **122**, 11571 (2000).
- [6] V. Petkov, S. J. L. Billinge, S. D. Shastri and B. Himmel, High-resolution atomic distribution functions of disordered materials by high-energy x-ray diffraction, *J. Non-Crystalline Solids* **293-295**, 726 (2000).
- [7] V. Petkov, S. J. L. Billinge, J. Heising, M. G. Kanatzidis, S. D. Shastri and S. Kycia, High real-space resolution structure of materials by high-energy x-ray diffraction, *Mater. Res. Soc. Symp. Proc.* **590**, 151 (2000).
- [8] V. Petkov, I.-K. Jeong, F. Mohiuddin-Jacobs, Th. Proffen and S. J. L. Billinge, Local structure of  $\text{In}_{0.5}\text{Ga}_{0.5}\text{As}$  from joint high-resolution and differential pair distribution function analysis, *J. Appl. Phys.* **88**, 665 (2000).
- [9] S. J. L. Billinge, Th. Proffen, V. Petkov, J. L. Sarrao and S. Kycia, Evidence for charge localization in the ferromagnetic phase of  $\text{La}_{1-x}\text{Ca}_x\text{MnO}_3$  from high real-space-resolution x-ray diffraction, *Phys. Rev. B* **62**, 1203 (2000).
- [10] V. Petkov, I.-K. Jeong, J. S. Chung, M. F. Thorpe, S. Kycia and S. J. L. Billinge, High real-space resolution measurement of the local structure of  $\text{Ga}_{1-x}\text{In}_x\text{As}$  using x-ray diffraction, *Phys. Rev. Lett.* **83**, 4089 (1999).
- [11] T. Egami, S. J. L. Billinge, S. Kycia, W. Dmowski and A. S. Eberhardt, Information stored in high Q-space: role of high energy scattering, *Nucl. Instr. and Methods* (1997).
- [12] B. E. Warren, *X-ray Diffraction*, Dover, New York, 1990.
- [13] A. M. Glass, *Science* **235**, 1003 (1985).
- [14] S. J. L. Billinge, P. F. Peterson, unpublished.
- [15] V. Petkov, S. J. L. Billinge, S. D. Shastri, and B. Himmel Polyhedral Units and Network Connectivity in Calcium Aluminosilicate Glasses from High-Energy X-Ray Diffraction *Phys. Rev. Lett.* **85**, 3436 (2000).
- [16] V. Petkov, S. J. L. Billinge, S. D. Mahanti, T. Vogt, K. K. Rangan and M. G. Kanatzidis, Structure of nanocrystalline materials using atomic pair distribution function analysis: study of  $\text{LiMoS}_2$ , *Phys. Rev. B* **65**, 092106 (2002).
- [17] V. Petkov, S. J. L. Billinge, T. Vogt, A. S. Ichimura, D. P. Wernette and J. L. Dye, *Phys. Rev. Lett.*, **89**, 075502 (2002); *Phys. Rev. Focus*, <http://focus.aps.org/v10/st4.html>